

## REVIEW ARTICLE

## A Critical Review of Echocardiographic Findings for Diagnosing Cardiac Amyloidosis

Silvio Henrique Barberato,<sup>1</sup> Adenalva Lima de Souza Beck,<sup>2,3</sup> Viviane Tiemi Hotta,<sup>4</sup> Daniela do Carmo Rassi<sup>5</sup>*Cardioeco, Centro de Diagnóstico Cardiovascular,<sup>1</sup> Curitiba, PR – Brazil**Instituto de Cardiologia e Transplantes do Distrito Federal (ICTDF-DF),<sup>2</sup> Brasília, DF – Brazil**Hospital Sírio Libanês,<sup>3</sup> Brasília, DF – Brazil**Instituto do Coração HC-FMUSP, Unidade Clínica de Miocardiopatias e Doenças da Aorta,<sup>4</sup> São Paulo, SP – Brazil**Faculdade de Medicina da Universidade Federal de Goiás,<sup>5</sup> Goiânia, GO – Brazil*

### Abstract

This article provides a critical review of the diagnostic value of several echocardiographic findings in cardiac amyloidosis (CA). The importance of early and accurate detection of CA is emphasized, considering its challenging diagnosis and the need for a high index of suspicion by clinicians. Echocardiography is often the first choice for imaging assessment of cardiac structure and function when CA is suspected. The article encompasses several conventional echocardiographic features and speckle-tracking echocardiography-derived deformation parameters. Some of these indexes are grouped together to form scores, which can improve the accuracy of diagnosing CA. However, particularly in earlier stages, echocardiography has low specificity to distinguish amyloid from other hypertrophic phenotypes, highlighting the need for correlation with clinical red flags, laboratory tests, and additional cardiac imaging modalities.

### Introduction

Cardiac amyloidosis (CA) is an infiltrative cardiomyopathy (CM) caused by the extracellular deposition of insoluble amyloid fibrils in the myocardium.<sup>1</sup> The two most common types of amyloid fibrils are (a) misfolded transthyretin (TTR), which can be either mutant (TTRm) or wild-type (TTRwt), (b)

and immunoglobulin light-chain (AL). Although the classic phenotype of unexplained left ventricular (LV) hypertrophy (LVH) and heart failure with preserved ejection fraction (HFpEF) has been widely reported,<sup>2</sup> CA is still an underdiagnosed disease due to the nonspecific nature of symptoms and limited awareness among physicians. Early, accurate diagnosis is crucial, as untreated CA patients have poor outcomes, and there are now effective treatment options available.

Echocardiography is the first-line screening tool for diagnosing CA.<sup>3</sup> An inexplicably increased LV wall thickness (“pseudohypertrophy”) often raises suspicion of the disease, particularly when associated with other clinical and echocardiographic red flags.<sup>3,4</sup> While conventional echocardiographic findings are often nonspecific, bidimensional speckle-tracking echocardiography (2D-STE) has been shown to identify a characteristic “apical sparing” (APS, or relative preservation of apical longitudinal strain compared to basal and mid-LV longitudinal strain) pattern associated with CA.<sup>5</sup> Other 2D-STE-derived deformation indexes have also been considered valuable in diagnosing CA.<sup>6,7</sup> However, recent research has highlighted the limitations of relying solely on single parameters, such as APS, as accurate diagnostic markers for CA in unselected patient populations.<sup>8-10</sup> One crucial point is that the echocardiographic parameters used to diagnose CA may not always change linearly or simultaneously (Central Illustration). The combination of changes depends on the time of onset and severity of CA. This article critically reviews the diagnostic yield of several traditional and novel echocardiographic findings in CA.

### Keywords

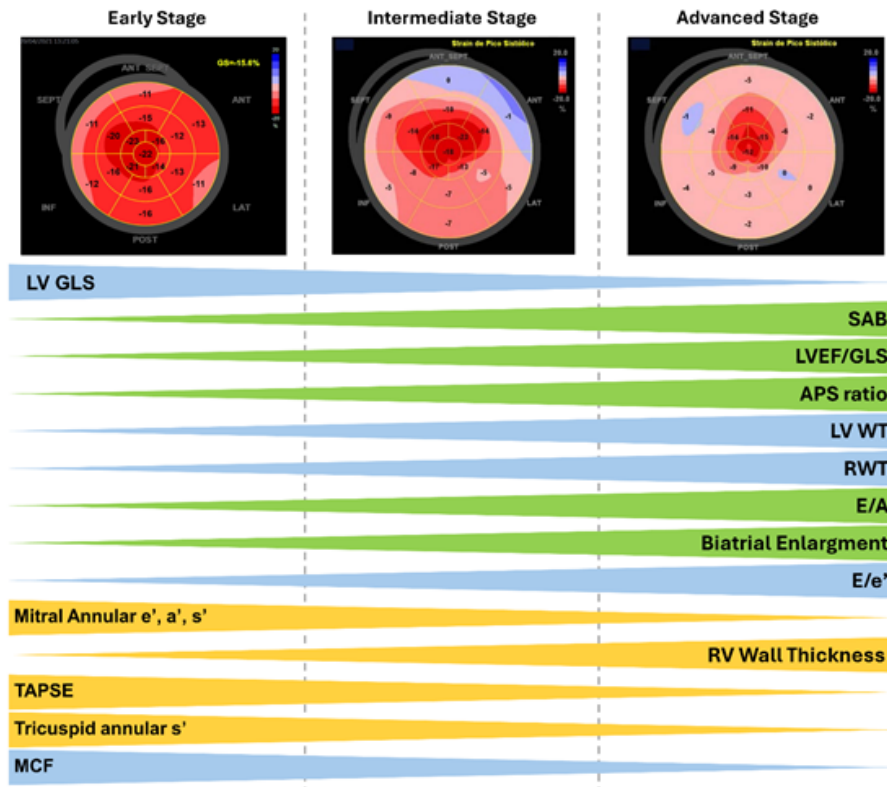
Amyloidosis; Echocardiography; Global Longitudinal Strain.

**Mailing Address: Silvio Henrique Barberato**

Cardioeco, Centro de Diagnóstico Cardiovascular. Avenida República Argentina, 1336, conj 215. Postal code: 80620-010. Curitiba, PR – Brazil

E-mail: silviohb@cardiol.br

Editor responsible for the review: Marcus Vinicius Simoes

**Central Illustration:** A Critical Review of Echocardiographic Findings for Diagnosing Cardiac Amyloidosis**MULTIPARAMETRIC APPROACH FOR THE DIAGNOSIS OF CARDIAC AMYLOIDOSIS**

Int J Cardiovasc Sci. 2024; 37:e20240047

Temporal evolution of changes in echocardiographic parameters used in the diagnosis of CA. Blue indexes represent early changes, green indexes represent intermediate changes, and orange indexes represent later changes in amyloid infiltration. LV: left ventricular; GLS: global longitudinal strain; SAB: septal apical to base strain; LVEF: Left ventricle ejection fraction; APS: apical sparing, or ratio of average apical longitudinal/average of base and mid longitudinal strain; WT: wall thickness; RWT: relative wall thickness; RV: right ventricular; TAPSE: tricuspid annular plane systolic excursion; MCF: myocardial contraction fraction;

## Clinical diagnosis

The clinician should maintain a high index of suspicion of CA, considering symptoms, age at onset, personal and family history, and specific clinical markers, known as red flags. In patients over 60 years of age, ATTR or AL amyloidosis should be investigated in the presence of carpal tunnel syndrome, unprovoked biceps tendon rupture (Popeye sign), back pain (spinal stenosis), polyneuropathy (neuropathic pain, difficulty walking, falls), intolerance to antihypertensive or heart failure medications (postural hypotension), HFpEF, and bradyarrhythmia.<sup>1</sup>

Clinical data alone cannot differentiate CA from other causes of restrictive cardiomyopathy (CM), and hence, further diagnostic tests, such as electrocardiography (ECG), laboratory exams, and cardiac imaging, are

necessary to confirm the underlying cause. Although ECG findings are nonspecific, low QRS voltage (or disproportionate LV wall thickness to QRS voltage), atrioventricular block, and pseudo-infarction pattern can be clues to underlying CA. In the appropriate context, such as in a hypertrophic phenotype, disproportionately high levels of NT-proBNP and chronic low-level elevation in serum troponin may suggest the diagnosis of CA. Likewise, abnormal free light chains ratio and positive serum and urine immunofixation are consistent with the diagnosis of AL amyloidosis.<sup>11</sup> Echocardiography is the first-choice imaging test, suggesting CA in a scenario of unexplained LV wall thickening, advanced diastolic dysfunction, and preserved ejection fraction (EF). However, classic echocardiographic features lack specificity to distinguish amyloid CM from other

hypertrophic phenotypes, such as nonamyloid infiltrative diseases and sarcomeric hypertrophic cardiomyopathy (HCM). Differential diagnosis of CA often demands a workup that includes 2D-STE-derived deformation indexes, cardiac magnetic resonance (CMR), technetium-99m- pyrophosphate bone scintigraphy (Tc99-PYP), and sometimes endomyocardial biopsy.<sup>12</sup> A comprehensive clinical judgment and individualized patient assessment remain central to rationalizing proper diagnostic tools.

### Conventional echocardiographic findings

CA should be suspected whenever there is an increase in LV wall thickness  $\geq 12$ mm on an echocardiogram, mainly in the absence of other justifying causes or if this finding is disproportionate to the cause (e.g., well-controlled arterial hypertension).<sup>4</sup> In the early stages of the disease, this “pseudohypertrophy” may be the only echocardiographic change. On the other hand, a normal LV wall thickness does not rule out CA.<sup>13</sup> Increased LV wall thickness is a nonspecific finding and requires careful clinical interpretation. Augmented myocardial walls associated with specific clinical conditions, such as HFpEF, degenerative aortic stenosis (AS), or HCM

starting after 65 years of age should raise suspicion of CA as an underlying cause.<sup>1</sup> As the disease progresses, additional findings make this hypothesis more likely, such as typical increased myocardial echogenicity, increased right ventricular (RV) wall thickness, thickening of the heart valves and interatrial septum, biatrial dilation, and pericardial and pleural effusion (Figure 1). In the more advanced phase, an infiltrative restrictive CM becomes evident.<sup>12</sup> These findings are summarized in Table 1 and detailed below.

The “typical” increased myocardial echogenicity (“speckling,” “sparkling,” hyperreflective “texture” of the myocardium) described in CA is neither specific nor sensitive for amyloidosis as it can occur in other causes of hypertrophy such as end-stage renal disease and other infiltrative cardiomyopathies. It raises the suspicion of CA when in combination with a severely reduced longitudinal function of the LV. Nevertheless, it can only be considered when using standard echocardiography imaging with no harmonic imaging.<sup>13</sup>

Although LV ejection fraction (LVEF) is usually preserved until advanced stages of disease, LV longitudinal systolic function is typically reduced early

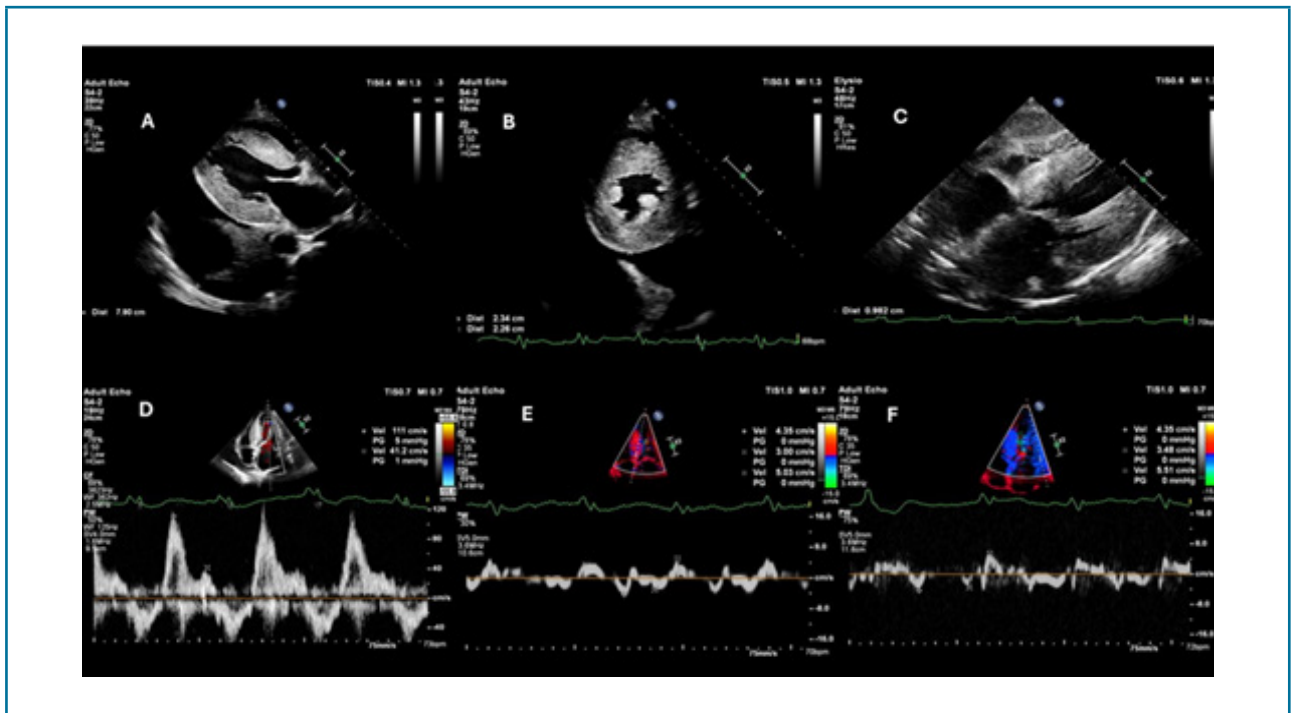


Figure 1 – Conventional echocardiographic findings suggestive of CA in a 71-year-old patient with arterial hypertension and previous myocardial revascularization admitted with HFpEF. Increased LV wall thickness (A and B), pleural effusion (A), interatrial septum thickening (c), LV diastolic dysfunction with a restrictive pattern (E/A 2.7, average E/e' 25.8) (D, E, and F) and “triple 5” sign (E). This patient was diagnosed with light chain amyloidosis, confirmed by anatomopathological examination of bone marrow biopsy

**Table 1 – Relative utility of echocardiographic parameters for the diagnosis of CA**

Echocardiographic parameter	Abnormal	Practical points	Caveats
<b>Conventional findings</b>			
LV WT	Increased ( $\geq 12$ mm) in the absence of a plausible cause	Disproportionate wall thickening in the absence of high ECG voltage is suggestive of CA.	Low specificity. If normal, it does not rule out CA.
RWT	$>0.42$	“Typical” concentric LV remodeling in opposition to eccentric or asymmetric. RWT is part of the multiparametric IWT and AL scores.	Asymmetry does not rule out CA
Myocardial echogenicity	Increased (granular “sparkling” appearance)	Only valid when not using harmonic imaging in the echocardiogram. Highly suggestive in conjunction with severely reduced GLS.	Low sensitivity and specificity. It can occur in other causes of hypertrophy.
RV “hypertrophy” and dysfunction	Increased free RV WT ( $> 7$ mm). Decreases in TAPSE ( $< 16$ mm) and tricuspid TDI $s' < 10$ cm/s)	Increased WT occurs in intermediate stages. RV dysfunction can occur before evidence of LV involvement	Low specificity
Atrial size and function	Atrial enlargement and dysfunction	Provides insight into risk for stroke or arterial embolism.	Low specificity
Interatrial septum and Cardiac valves	Thickening of the interatrial septum ( $> 5$ mm) and valves	Suggestive of the diagnosis, especially if along with myocardial “sparkling”.	Low specificity
Pericardial effusion	Often mild effusion	Suggestive of the diagnosis when accompanied by other typical findings.	Low specificity
Diastolic dysfunction	Typically, grade $\geq$ II diastolic dysfunction	Early stage: average $E/e' > 13$ is one of the first echocardiographic signs of CA. Later stage: restrictive physiology. Correlate with severity of symptoms and prognosis.	Low specificity
TDI of mitral annulus	The “5-5-5” sign	Highly suggestive of the diagnosis.	Low sensitivity in early stages
MCF	20–30%	Independent of chamber size and geometry. It appears to have the best diagnostic performance among non-deformation parameters.	Validation only in TTR-CA
<b>Speckle-tracking echocardiography</b>			
LV GLS	$< 16$	Sensitive marker of subclinical dysfunction. CA patients tend to have lower GLS values than HCM patients with similar LV wall thickness. GLS is part of the multiparametric IWT and AL scores.	Non-specific
APS ratio	$>1$	Relative preservation of apical LS compared to basal and mid-LV LS (“cherry-on-top” sign on the bullseye map).	APS can be found in other hypertrophic phenotypes in the absence of CA and even in healthy subjects.
SAB	$>2.1$	SAB is part of the multiparametric IWT score.	Modest accuracy in real-world cohorts
LVEF/GLS	$>4.1$	Highest accuracy for the diagnosis of CA in comparison to APS and SAB	Modest accuracy in real-world cohorts
<p><i>LV: left ventricular; WT: wall thickness; ECG: electrocardiography; CA: cardiac amyloidosis; RWT: relative wall thickness; RV: right ventricular; TAPSE: tricuspid annular plane systolic excursion; LVH: LV hypertrophy; TDI: tissue Doppler imaging; MCF: myocardial contraction fraction; ATTR: transthyretin amyloidosis; APS: apical sparing, or ratio of average apical longitudinal/average of base and mid longitudinal strain; SAB: septal apical to base strain; IWT: increased wall thickness; AL: light-chain; GLS: global longitudinal strain; RV: right ventricle; LVEF: Left ventricle ejection fraction. Adapted and expanded from Cuddy et al.<sup>13</sup></i></p>			

on despite normal LVEF. Tissue Doppler Imaging (TDI) can measure regional myocardial velocities and detect longitudinal systolic and diastolic function changes before LVEF drops. Systolic ( $s'$ ) and diastolic velocities ( $e'$  and  $a'$ ) derived from TDI of septal and lateral mitral annulus are reduced in CA. The "5-5-5" sign (all three velocities  $< 5\text{cm/s}$  on mitral annulus TDI) is highly suggestive of CA but only evident in advanced stages of the disease (Figure 1).<sup>13</sup>

RV infiltration is common in CA patients, leading to "hypertrophy" (RV free wall  $> 7\text{mm}$ ) and dysfunction, as evidenced by decreases in tricuspid annular plane systolic excursion (TAPSE) ( $< 16\text{mm}$ ) and tricuspid TDI systolic velocity ( $s' < 10\text{cm/s}$ ).<sup>14,15</sup>

Diastolic dysfunction is a hallmark of CA, clinically ranging from absence of symptoms and abnormal relaxation to restrictive physiology. In earlier stages, grade I or II diastolic dysfunction may be present. An average septal and lateral mitral annulus  $E/e' > 13$  is one of the first echocardiographic signs of CA (Central Illustration).<sup>16</sup> Assessment of pulmonary vein atrial reversal may suggest increased LV end-diastolic pressure and atrial function. These features usually manifest after an increase in LV wall thickness but sometimes can be observed even before an overt increase in myocardial wall.<sup>17</sup> In advanced CA, a restrictive pattern of diastolic dysfunction can be observed due to stiffening of the myocardium by amyloid infiltration. Restrictive physiology is characterized by  $E/A$  ratio  $> 2$ , low  $e'$  (usually  $< 6\text{cm/s}$ ),  $E/e'$  ratio  $> 15$ , short deceleration time of diastolic mitral valve inflow (also of prognostic significance if  $< 150\text{ms}$ ), systolic blunting of pulmonary vein flow, and bi-atrial dilation.<sup>18</sup> Enlarged atria, often immobile, with an "owl's eyes" appearance, are common in CA and reflect increased LV filling pressures. Severely reduced A wave velocity, particularly in the absence of other features of restrictive LV filling, is a clue to atrial dysfunction and a predictor of risk of stroke even in the setting of normal sinus rhythm.<sup>14</sup>

Amyloid deposition can cause thickening of the interatrial septum ( $> 5\text{mm}$  in atrial diastole) and thickening of the aortic, mitral, and tricuspid valves.<sup>15</sup> Although these findings are nonspecific, they should raise suspicion for CA in the proper clinical context.<sup>18</sup>

Small pericardial or pleural effusions are common in CA. Pericardial effusion is present in more than 50% of patients with CA. While these features may not have high specificity, they can still suggest the diagnosis.<sup>19</sup>

## Relative wall thickness (RWT)

RWT helps to categorize LV remodeling/hypertrophy into concentric ( $> 0.42$ ) or eccentric ( $\leq 0.42$ ). It contributes to calculating validated echocardiographic scores in diagnosing CA,<sup>20</sup> but should be interpreted cautiously. Although CA patients are thought to have concentric remodeling, a feature commonly observed in AL-CA, many patients exhibit increased wall thickness (IWT) in TTR-CA with a predominance of asymmetric septum. This parameter has been evaluated in clinical investigations using two approaches:  $RWT = 2 * \text{posterior wall dimension (PWd)} / \text{LV dimension (LVIDd)}$  or  $RWT = \text{interventricular septum dimension (IVSd)} + \text{PWd} / \text{LVIDd}$ . The British Society of Echocardiography recommends using the latter formula, as relying only on posterior wall thickness may underestimate the RWT in many patients with TTR-CA.<sup>18</sup> In a CMR study involving individuals with TTR-CA, 79% showed asymmetrical hypertrophy, while only 18% were categorized as having concentric wall thickening. Most patients with TTR-CA and a septal/lateral wall thickness ratio exceeding 1.5 showed a sigmoidal septal remodeling pattern. Still, almost a quarter of them had a reverse septal curvature, which is typically linked to HCM.<sup>21</sup>

## Myocardial contraction fraction (MCF)

MCF is the stroke volume/LV volume ratio that can evaluate the myocardial contraction capacity of CA patients and help differentiate CA from LVH caused by other diseases. For example, the values range from 30–45% in patients with HFpEF induced by systemic inflammation or metabolic diseases, 35–45% in patients with HCM, and 20–30% in CA patients.<sup>20</sup> This measurement demonstrated high diagnostic accuracy in an echocardiography study of patients with TTR-CA (AUC = 0.80). As myocardial amyloid accumulation progresses over time, it leads to an increase in myocardial mass and a decrease in ventricular cavity size, ultimately resulting in stroke volume reduction. This may lead to a condition characterized by a consistent reduction in end-diastolic volume, where the cardiac output becomes highly dependent on heart rate. This is exacerbated by the infiltration of amyloid into the valves, causing mitral and tricuspid regurgitation, further affecting the forward stroke volume.<sup>22</sup> Among non-deformation parameters, MCF appears to have the best diagnostic performance, at least in TTR-CA patients.<sup>22</sup>

## Speckle-tracking echocardiography

Strain analysis plays a fundamental role in the echocardiographic evaluation of patients with suspected CA. 2D-STE enables the study of myocardial strain (deformation) through the tracking of natural acoustic markers ("speckles") in the myocardium. Dedicated software tracks the displacement of the speckles through the cardiac cycle and calculates the relative myocardial deformation or strain rate. This technique allows global or segmental longitudinal, circumferential, and radial strain analysis.

The most robust and extensively validated parameter in clinical studies is LV global longitudinal strain (GLS), which may be altered before changes in EF.<sup>23</sup> This is explained by the fact that longitudinal myocardial fibers are located in the subendocardium and represent the majority of the fibers, which are early affected in ischemia or other myocardial injuries. In patients with CA, myocardial deformation indexes derived from strain analysis can be helpful in the differential diagnosis of LVH, particularly in patients with HFpEF at the early disease stages.<sup>15</sup> GLS is an early marker of subclinical dysfunction, which can be reduced even before the onset of LV myocardial thickening in patients with CA. Furthermore, compared to HCM patients with similar LV wall thickness, CA patients have lower GLS values.<sup>24</sup>

In 2012, Phelan et al.<sup>5</sup> described a regional pattern of relative APS of longitudinal strain compared to basal and mid-LV longitudinal strain, resulting in the so-called "APS pattern" on the polar map (Figure 2). Apical longitudinal strain divided by the sum of base and mid longitudinal strain (relative regional strain ratio)  $\geq 1$  was 93% sensitive and 82% specific for differentiating CA from other causes of LVH, such as HCM and AS.<sup>5</sup> However, this was a single-center study with a highly selected population and a small sample size (N = 55). In addition, although APS was initially thought to be specific for CA, it can also be found in patients with severe chronic kidney disease,<sup>25</sup> AS,<sup>10</sup> and hypertensive CM<sup>9</sup> in the absence of CA. In 2013, Liu et al.<sup>6</sup> concluded that a septal apical-to-basal longitudinal strain (SAB) ratio  $>2.1$ , combined with a shortened mitral E wave deceleration time  $<200$  milliseconds, helps differentiate CA from other causes of concentric LVH, such as isolated arterial hypertension, Fabry disease, and Friedreich ataxia. In 2016, Pagourelias et al.<sup>7</sup> introduced a novel index, the LVEF/GLS ratio, which

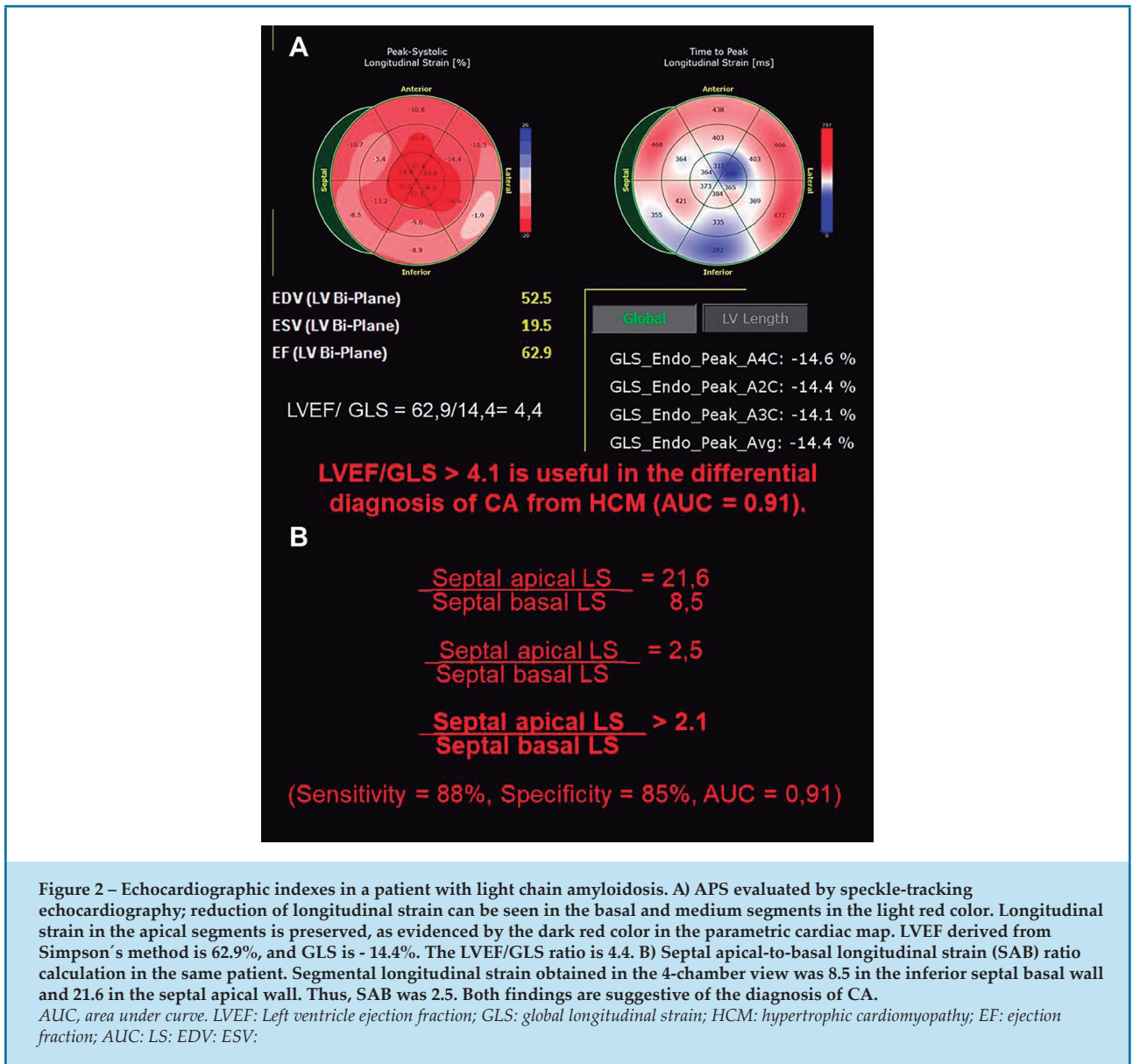
was significantly higher among CA patients than in other groups.<sup>7</sup> Receiver operator analysis showed an optimal cutoff value of  $> 4.1$  to differentiate CA from HCM (area under the curve, or AUC, 0.91).

Given the several echocardiographic parameters described, some studies were conducted to compare the diagnostic accuracy of deformation and non-deformation variables in differentiating CA from other hypertrophic phenotypes and controls. Pagourelias et al.<sup>26</sup> compared different methods for measuring myocardial deformation in 40 patients with confirmed CA, 40 with CMH, and 20 with arterial hypertension. The study found that LVEF/GLS  $> 4.1$  had the highest accuracy in diagnosing CA, with a sensitivity of 89.7% and specificity of 91.7%. LVEF/GLS remained the most reliable parameter for predicting CA diagnosis, irrespective of the CA type, and even in the challenging subgroups with mild LVH and normal EF. Other conventional echocardiographic indexes showed overall low sensitivity.<sup>26</sup> Another study with 100 patients who underwent complete cardiac evaluation for CA showed that both SAB (AUC 0.72) and LVEF/GLS (AUC 0.72) improved discrimination of CA compared with the visual assessment of APS (AUC 0.66).<sup>8</sup>

A retrospective study conducted by Wali et al.<sup>9</sup> with a small sample of patients assessed the frequency at which APS indicated the presence of CA and revealed that this occurred in only one-third of cases. The probability of APS indicating CA is higher in elderly patients with greater LV wall thickness.<sup>9</sup> Consequently, many patients with APS may show no evidence of CA in further investigations.

In one of the largest cohorts of CA patients reported in the literature, including a control group with clinically similar findings but excluding CA, Cotella et al.<sup>10</sup> showed that APS was present in about one-third of non-CA patients with similar clinical presentation and even in 1/10 of the healthy subjects. The study unveiled that even when using a different optimal cutoff ( $> 1.67$ ) from the original study by Phelan et al.,<sup>5</sup> APS had relatively poor diagnostic accuracy in a large cohort of patients with or without CA.

Evaluation of right cardiac chambers in patients with CA has evidenced that RV involvement is not uncommon. RV-APS pattern has been described in patients with TTR-CA.<sup>27</sup> It has been suggested that RV dysfunction can occur before evidence of LV involvement and be used for early diagnosis of CA. In



addition, TAPSE and free wall RV longitudinal strain have been associated with a worse prognosis.<sup>28</sup>

### Echocardiographic scores

Previous studies have confirmed that various echocardiographic variables on their own are associated with different levels of diagnostic accuracy in CA. However, combining parameters that reflect both structural and functional changes can improve the accuracy of echocardiography in diagnosing CA in certain situations.

In 2020, Boldrini et al.<sup>29</sup> assessed the accuracy of a multiparametric echocardiographic approach to diagnose

CA in patients with proven AL amyloidosis and in those with increased LV wall thickness suspected of having amyloidosis. To develop a score-based diagnostic algorithm, 332 patients with AL and 339 patients with TTR-CA were analyzed for morphological, functional, and strain-derived parameters on echocardiography (Table 2). Cardiac amyloid burden was quantified using extracellular volume measurements on CMR. For individuals with LV wall thickening, an IWT score, calculated using RWT, E/e’ ratio, TAPSE, GLS, and SAB, offered a high level of diagnostic accuracy for TTR-CA (≥ 8 points resulting in an AUC of 0.87). In AL amyloidosis, an AL score ≥ 5 points derived from RWT, E/e’ ratio, GLS,

**Table 2 – Variable cut-Offs for calculation of the AL and IWT scores**

	Cut-Off	Points
<b>AL score: indicative of AL-CA if <math>\geq 5</math> points</b>		
RWT	$>0,52$	2
E/e'	$>10$	2
TAPSE, mm	$\leq 19$	1
GLS, %	$\geq - 14$	1
<b>IWT score: indicative of TTR-CA if <math>\geq 8</math> points</b>		
RWT	$>0,6$	3
E/e'	$>11$	1
TAPSE, mm	$\leq 19$	2
GLS, %	$\geq - 13$	1
SAB	$>2,9$	2

*AL: light-chain; IWT: increased wall thickness; CA: cardiac amyloidosis; RWT: relative wall thickness; E/e': ratio of the early (E) to late (A) ventricular filling velocities; TAPSE: tricuspid annular plane systolic excursion; GLS: global longitudinal strain; SAB: septal apical-to-basal longitudinal strain ratio; adapted from Boldrini et al.<sup>29</sup>*

and TAPSE also demonstrated outstanding diagnostic performance in discriminating patients with AL-CA, with an AUC of 0.90. Although this proposed scoring system, which utilizes specific echocardiographic parameters, has not undergone external validation, the European Society of Cardiology has endorsed it to assist in the diagnosis of CA.<sup>4</sup> The AL and IWT scores yield good diagnostic accuracy and may help clinicians in determining whether additional tests like CMR or Tc99-PYP and even endomyocardial biopsy are needed. On the other hand, there are potential limitations in using two scoring systems. First, strain assessment may not be routine in all echocardiography laboratories. Second, distinct equations are used to calculate the scores, which may lead to confusion. Lastly, there are no clearly defined thresholds for ruling out or confirming CA.

In 2021, Aimo et al.<sup>30</sup> aimed to address these limitations by developing a simplified scoring system for diagnosing AL- and TTR-CA. The amyloidosis index (AMYLI score) incorporates only two commonly available variables – the product of RWT and E/e' ratio – and establishes setting-specific thresholds to exclude CA. In the original cohort of 251 patients, CA was diagnosed in 111 (44%). The threshold of 2.22 was established as the general rule-out cut-off. AL-CA was identified in 32 patients (48%) in the hematology subset, utilizing a rule-out cut-off of

2.36. TTR-CA was detected in 79 patients (43%) in the hypertrophy subset, with 2.22 as the optimal rule-out cut-off. These same cut-offs demonstrated effectiveness in the validation cohort, where  $<2.22$ ,  $<2.36$ , or  $<2.22$  values excluded the diagnosis in the entire population and in the hematology and hypertrophy subsets, respectively. Limitations of this study included the fact that the variables selected for the AMYLI score were chosen arbitrarily from the AL and IWT scores without a specific rationale. Moreover, multiplying these variables instead of giving them different weights and summing them was also arbitrary. The study population was analyzed retrospectively and partly overlapped with the one used to create the AL and IWT scores. However, the analysis of the AMYLI score was conducted independently and blinded to the previous scores. Finally, the prevalence of CA was notably high, particularly in the validation cohort, possibly due to referral patterns.

Patients with HFpEF are at a higher risk of having TTR-CA. To address this issue, Davies et al.<sup>31</sup> developed and validated an "ATTR-CM score" consisting of three clinical and three echocardiographic variables to predict TTR-CA risk in HFpEF cohorts with varying prevalence rates of TTR-CA. By using this score, clinicians can identify the need for Tc99-PYP and eventually provide appropriate therapy for TTR-CA in patients with HFpEF.



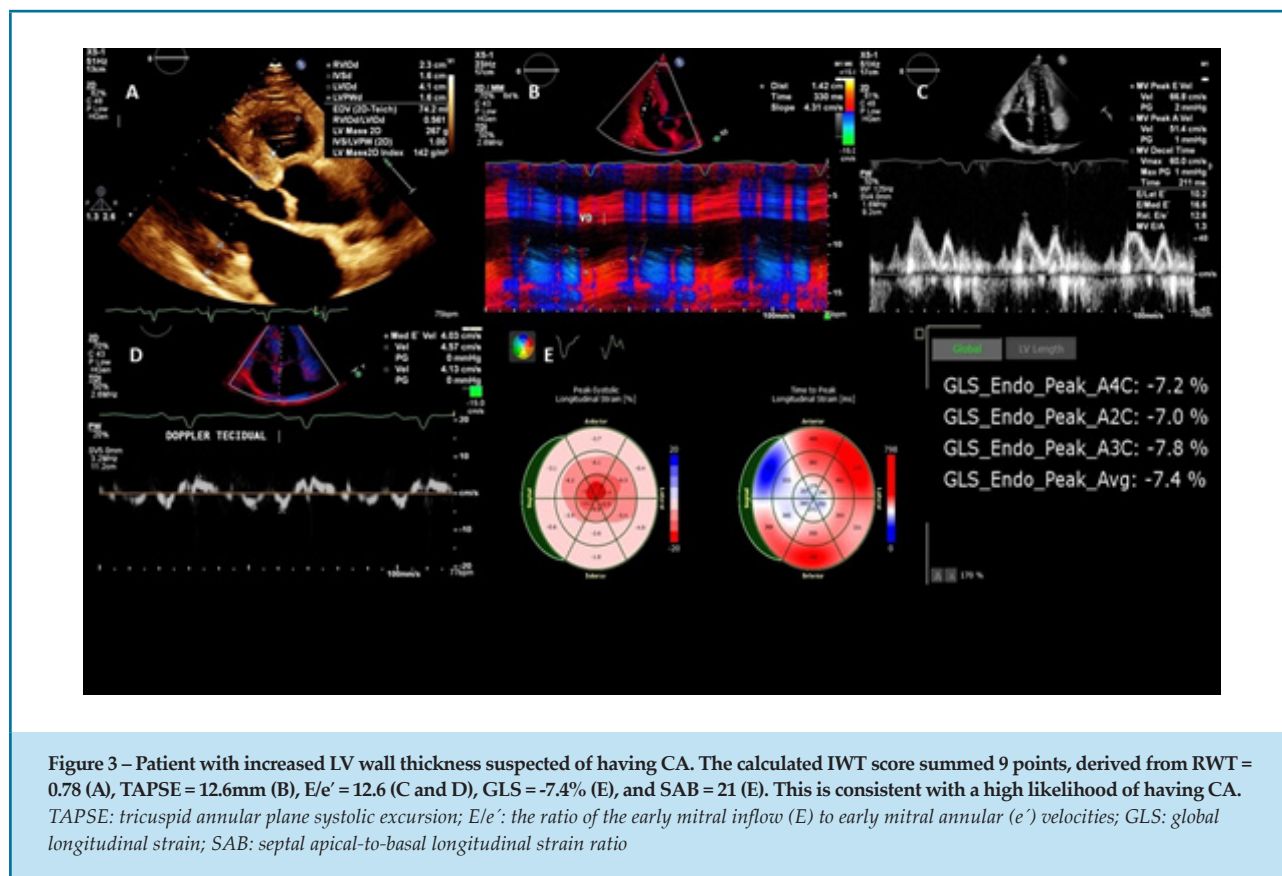


**Figure 3 – Patient with increased LV wall thickness suspected of having CA. The calculated IWT score summed 9 points, derived from RWT = 0.78 (A), TAPSE = 12.6mm (B), E/e' = 12.6 (C and D), GLS = -7.4% (E), and SAB = 21 (E). This is consistent with a high likelihood of having CA. TAPSE: tricuspid annular plane systolic excursion; E/e': the ratio of the early mitral inflow (E) to early mitral annular (e') velocities; GLS: global longitudinal strain; SAB: septal apical-to-basal longitudinal strain ratio**

Score variables included age (60–69: 2 points, 70–79: 3 points, ≥ 80: 4 points), male sex (2 points), hypertension diagnosis (-1 point), RWT greater than 0.57 (2 points), posterior wall thickness of 12 mm or more (1 point), and LVEF less than 60% (1 point). The study authors identified TTR-CA patients in the HFpEF group. They found that patients with 6 points or more had a high risk of CA with a positive predictive value (PPV) of 25% or greater. However, the "ATTR-CM score" was derived from patients already referred for Tc99-PYP imaging due to suspected TTR-CA, so its accuracy may vary when applied to patients with HFpEF in general. Additionally, the study did not have a diverse racial representation, and most participants were male.

Another scoring system was developed by Nakao et al.<sup>32</sup> to assess the value of APS combined with other variables in the diagnosis of CA. Through multivariate analysis, the study established four scoring criteria: 1 point for males aged over 65 years (females aged over 70 years), ECG low voltage in limb leads, LV posterior wall thickness of ≥ 14 mm, and APS. Over 60% of the subjects with 2 points were diagnosed with CA, and this percentage increased to 85% among patients with

3 points or more. APS exhibited the most significant incremental benefit for CA screening beyond the base model. The score showed adequate discrimination ability for CA (AUC = 0.86), which was corroborated in another validation cohort (AUC = 0.88). Limitations of the study were its retrospective design, incomplete laboratory data, unavailable strain analysis for some patients, and the use of different ultrasound machines, possibly affecting data reproducibility. Additionally, the score was more applicable to TTR-CA than AL-CA.

Finally, a score using biomarkers was developed by Nicol et al.<sup>33</sup> Cardiac involvement was determined by CMR and endomyocardial biopsy. The highest diagnostic accuracy was observed with NT-proBNP and troponin blood levels, GLS, and relative regional strain ratio (as a surrogate for APS) in a derivation cohort. A diagnostic score including global GLS ≥ -17% (1 point), apical/(basal + medium) LS ≥ 0.90 (1 point), and troponin T > 35 ng/L (1 point) was proposed, and a value > 1 was associated with sensitivity of 94% and specificity of 97% (AUC = 0.98). It is noteworthy that in multivariate analysis, the diagnostic accuracy of the LVEF/GLS ratio was lower than that of GLS and APS, which contrasts with the findings

of other studies.<sup>5,12</sup> Thus, the LVEF/GLS ratio was not included in the scoring algorithm. Also, GLS and APS were unavailable for a small number of patients.

### Artificial Intelligence (AI)

In recent years, AI has been widely applied and proved to be a promising approach in addressing various tasks related to medical imaging. Deep learning is an advanced machine learning method that can automatically extract features from large datasets to significantly enhance the performance of functions such as visual object recognition and detection. This can be crucial in echocardiography, particularly for diseases associated with LVH.<sup>34</sup> However, dependency on the operator's experience is high and may differ among echocardiographers. Some studies have shown promising results in using deep learning in echocardiography and CA. In a multi-center study, Goto et al.<sup>35</sup> applied an automatic CA detection model using ECG and echocardiography. Using ECG as a pre-screening tool elevated the recall rate of the echocardiography model by 67% and lifted the positive predictive value from 33 to 74–77%, including TTR-CA.<sup>35</sup> In another study, the same author evaluated the use of AI in improving hypertrophy detection performance in the ultrasound modality for the binary classification of HCM vs. other diseases.<sup>36</sup> The ECG and echocardiogram model trained with the federated learning approach showed good discrimination between HCM and other causes of LVH (hypertension, AS, and CA).<sup>36</sup> This suggests that the model could aid in detecting cases that are hard to detect without CMR. In another research, Huda et al.<sup>37</sup> identified TTR-CA patients with an AUC ranging from 0.76 to 0.95 by developing and validating an approach using machine learning. This result was based on medical claims data, which provided a systematic framework for screening and identifying potential wild-type TTR-CA patients.<sup>37</sup> To assess CA subtypes, Bonnefous et al.<sup>38</sup> used clustering analysis to identify typical clinical profiles in a large population of patients with suspected CA. AL patients were found in a typical cluster, while TTRm patients were distributed in four of the seven clusters with different clinical presentations. One of these clusters overlapped with patients without amyloidosis. Finally, TTRwt patients were found in three groups with distinct risk factors, biological profiles, and prognoses.<sup>38</sup> AI holds promise for enhancing the diagnosis and management of CA patients in the future. Research must focus on overcoming limitations and challenges to fully realize its potential. It is crucial to evaluate AI models prospectively

to ensure their successful integration into clinical practice and guide future research in this domain.

### Conclusions

Echocardiography remains the initial and pivotal cardiac imaging technique for patients with suspected CA. Conventional echocardiographic features and myocardial deformation parameters have been used to diagnose CA in patients with unexplained LVH. However, traditional bidimensional and Doppler echocardiographic findings are inaccurate in distinguishing CA from other hypertrophic phenotypes. 2D-STE-derived deformation indexes like APS, SAB, and especially LVEF/GLS have higher accuracy rates, while conventional parameters have low specificity,<sup>26</sup> particularly in the early stages. Regardless of the approach, there are limitations in using single echocardiographic variables as reliable biomarkers for detecting CA in the general population. Although APS and other deformation indexes are helpful for suggesting CA, they have modest sensitivity and specificity in real-world cohorts when used alone,<sup>10</sup> and none of these variables can differentiate between subtypes of CA. Additionally, other cardiomyopathies can mimic CA, leading to a significant overlap, which can further complicate the diagnosis. Combining deformation with conventional echocardiographic findings in patients suspected of having CA, ideally as early as possible, can improve diagnostic accuracy. Also, several scoring systems have been developed to improve the diagnosis of CA in patients with hypertrophic phenotypes, including multiparametric echocardiographic approaches such as the IWT and AL scores<sup>29</sup> and the AMYLI score,<sup>30</sup> the latter not requiring strain imaging. The body of evidence supports the role of these novel scores to enhance the diagnostic suspicion of CA in echocardiographic studies. There will be instances where echocardiography fails to differentiate between CA and other causes of “thick hearts.” In such scenarios, clinicians must carefully evaluate the sum of echocardiographic findings along with the patient's medical and family history, ECG, and blood tests and often conduct additional complementary cardiac imaging studies capable of tissue characterization, such as CMR and Tc<sup>99</sup>-PYP. In the near future, incorporating AI into noninvasive imaging and clinical data can improve diagnostic accuracy and refine clinical decision-making for CA patients.

## Author Contributions

Conception and design of the research: Barberato SH; acquisition of data, analysis and interpretation of the data, writing of the manuscript and critical revision of the manuscript for intellectual content: Barberato SH, Beck ALS, Hotta VT, Rassi DC.

### Potential Conflict of Interest

No potential conflict of interest relevant to this article was reported.

## References

1. Kittleson MM, Maurer MS, Ambardekar AV, Bullock-Palmer RP, Chang PP, Eisen HJ, et al. Cardiac Amyloidosis: Evolving Diagnosis and Management: A Scientific Statement from the American Heart Association. *Circulation*. 2020;142(1):e7-e22. doi: 10.1161/CIR.0000000000000792.
2. González-López E, Gallego-Delgado M, Guzzo-Merello G, de Haro-Del Moral FJ, Cobo-Marcos M, Robles C, et al. Wild-Type Transthyretin Amyloidosis as a Cause of Heart Failure with Preserved Ejection Fraction. *Eur Heart J*. 2015;36(38):2585-94. doi: 10.1093/eurheartj/ehv338.
3. Barberato SH, Romano MMD, Beck ALS, Rodrigues ACT, Almeida ALC, Assunção BMBL, et al. Position Statement on Indications of Echocardiography in Adults - 2019. *Arq Bras Cardiol*. 2019;113(1):135-81. doi: 10.5935/abc.20190129.
4. Garcia-Pavia P, Rapezzi C, Adler Y, Arad M, Basso C, Brucato A, et al. Diagnosis and Treatment of Cardiac Amyloidosis: A Position Statement of the ESC Working Group on Myocardial and Pericardial Diseases. *Eur Heart J*. 2021;42(16):1554-68. doi: 10.1093/eurheartj/ehab072.
5. Phelan D, Collier P, Thavendiranathan P, Popović ZB, Hanna M, Plana JC, et al. Relative Apical Sparing of Longitudinal Strain Using Two-Dimensional Speckle-Tracking Echocardiography is Both Sensitive and Specific for the Diagnosis of Cardiac Amyloidosis. *Heart*. 2012;98(19):1442-8. doi: 10.1136/heartjnl-2012-302353.
6. Liu D, Hu K, Niemann M, Herrmann S, Cikes M, Störk S, et al. Effect of Combined Systolic and Diastolic Functional Parameter Assessment for Differentiation of Cardiac Amyloidosis from Other Causes of Concentric Left Ventricular Hypertrophy. *Circ Cardiovasc Imaging*. 2013;6(6):1066-72. doi: 10.1161/CIRCIMAGING.113.000683.
7. Pagourelas ED, Duchenne J, Mirea O, Vovas G, Van Cleemput J, Delforge M, et al. The Relation of Ejection Fraction and Global Longitudinal Strain in Amyloidosis: Implications for Differential Diagnosis. *JACC Cardiovasc Imaging*. 2016;9(11):1358-9. doi: 10.1016/j.jcmg.2015.11.013.
8. Kyrouac D, Schiffer W, Lennep B, Fergestrom N, Zhang KW, Gorcsan J 3rd, et al. Echocardiographic and Clinical Predictors of Cardiac Amyloidosis: Limitations of Apical Sparing. *ESC Heart Fail*. 2022;9(1):385-97. doi: 10.1002/ehf2.13738.
9. Wali E, Gruca M, Singulane C, Cotella J, Guile B, Johnson R, et al. How Often Does Apical Sparing of Longitudinal Strain Indicate the Presence of Cardiac Amyloidosis? *Am J Cardiol*. 2023;202:12-6. doi: 10.1016/j.amjcard.2023.06.022.
10. Cotella J, Randazzo M, Maurer MS, Helmke S, Scherrer-Crosbie M, Soltani M, et al. Limitations of Apical Sparing Pattern in Cardiac Amyloidosis: A Multicenter Echocardiographic Study. *Eur Heart J Cardiovasc Imaging*. 2024;jeae021. doi: 10.1093/ehjci/jeae021.
11. Arbelo E, Protonotarios A, Gimeno JR, Arbustini E, Barriales-Villa R, Basso C, et al. 2023 ESC Guidelines for the Management of Cardiomyopathies. *Eur Heart J*. 2023;44(37):3503-626. doi: 10.1093/eurheartj/ehad194.

## Sources of Funding

There were no external funding sources for this study.

## Study Association

This study is not associated with any thesis or dissertation work.

## Ethics Approval and Consent to Participate

This article does not contain any studies with human participants or animals performed by any of the authors.

12. Simões MV, Fernandes F, Marcondes-Braga FG, Scheinberg P, Correia EB, Rohde LEP, et al. Position Statement on Diagnosis and Treatment of Cardiac Amyloidosis - 2021. *Arq Bras Cardiol*. 2021;117(3):561-98. doi: 10.36660/abc.20210718.
13. Cuddy SAM, Chetrit M, Jankowski M, Desai M, Falk RH, Weiner RB, et al. Practical Points for Echocardiography in Cardiac Amyloidosis. *J Am Soc Echocardiogr*. 2022;35(9):A31-A40. doi: 10.1016/j.echo.2022.06.006.
14. Dorbala S, Cuddy S, Falk RH. How to Image Cardiac Amyloidosis: A Practical Approach. *JACC Cardiovasc Imaging*. 2020;13(6):1368-83. doi: 10.1016/j.jcmg.2019.07.015.
15. Moura B, Aimo A, Al-Mohammad A, Keramida K, Ben Gal T, Dorbala S, et al. Diagnosis and Management of Patients with Left Ventricular Hypertrophy: Role of Multimodality Cardiac Imaging. A Scientific Statement of the Heart Failure Association of the European Society of Cardiology. *Eur J Heart Fail*. 2023;25(9):1493-506. doi: 10.1002/ehf.2997.
16. Knight DS, Zumbo G, Barcella W, Steeden JA, Muthurangu V, Martinez-Naharro A, et al. Cardiac Structural and Functional Consequences of Amyloid Deposition by Cardiac Magnetic Resonance and Echocardiography and Their Prognostic Roles. *JACC Cardiovasc Imaging*. 2019;12(5):823-33. doi: 10.1016/j.jcmg.2018.02.016.
17. Dorbala S, Ando Y, Bokhari S, Dispenzieri A, Falk RH, Ferrari VA, et al. ASNC/AHA/ASE/EANM/HFSA/ISA/SCMR/SNMMI Expert Consensus Recommendations for Multimodality Imaging in Cardiac Amyloidosis: Part 1 of 2-Evidence Base and Standardized Methods of Imaging. *J Nucl Cardiol*. 2019;26(6):2065-123. doi: 10.1007/s12350-019-01760-6.
18. Moody WE, Turvey-Haigh L, Knight D, Coats CJ, Cooper RM, Schofield R, et al. British Society of Echocardiography Guideline for the Transthoracic Echocardiographic Assessment of Cardiac Amyloidosis. *Echo Res Pract*. 2023;10(1):13. doi: 10.1186/s44156-023-00028-7.
19. Binder C, Duca F, Binder T, Rettl R, Dachs TM, Seirer B, et al. Prognostic Implications of Pericardial and Pleural Effusion in Patients with Cardiac Amyloidosis. *Clin Res Cardiol*. 2021;110(4):532-43. doi: 10.1007/s00392-020-01698-7.
20. Maurer MS, Packer M. How Should Physicians Assess Myocardial Contraction?: Redefining Heart Failure with a Preserved Ejection Fraction. *JACC Cardiovasc Imaging*. 2020;13(3):873-8. doi: 10.1016/j.jcmg.2019.12.021.
21. Martinez-Naharro A, Treibel TA, Abdel-Gadir A, Bulluck H, Zumbo G, Knight DS, et al. Magnetic Resonance in Transthyretin Cardiac Amyloidosis. *J Am Coll Cardiol*. 2017;70(4):466-77. doi: 10.1016/j.jacc.2017.05.053.
22. Chacko L, Martone R, Bandera F, Lane T, Martinez-Naharro A, Boldrini M, et al. Echocardiographic Phenotype and Prognosis in Transthyretin Cardiac Amyloidosis. *Eur Heart J*. 2020;41(14):1439-47. doi: 10.1093/eurheartj/ehz905.

23. Almeida ALC, Melo MDT, Bihan DCSL, Vieira MLC, Pena JLB, Del Castillo JM, et al. Position Statement on the Use of Myocardial Strain in Cardiology Routines by the Brazilian Society of Cardiology's Department Of Cardiovascular Imaging - 2023. *Arq Bras Cardiol.* 2023;120(12):e20230646. doi: 10.36660/abc.20230646.
24. Pagourelas ED, Mirea O, Vovas G, Duchenne J, Michalski B, Van Cleemput J, et al. Relation of Regional Myocardial Structure and Function in Hypertrophic Cardiomyopathy and Amyloidosis: A Combined Two-Dimensional Speckle Tracking and Cardiovascular Magnetic Resonance Analysis. *Eur Heart J Cardiovasc Imaging.* 2019;20(4):426-37. doi: 10.1093/ehjci/jej107.
25. Singh V, Soman P, Malhotra S. Reduced Diagnostic Accuracy of Apical-Sparing Strain Abnormality for Cardiac Amyloidosis in Patients with Chronic Kidney Disease. *J Am Soc Echocardiogr.* 2020;33(7):913-6. doi: 10.1016/j.echo.2020.03.012.
26. Pagourelas ED, Mirea O, Duchenne J, Van Cleemput J, Delforge M, Bogaert J, et al. Echo Parameters for Differential Diagnosis in Cardiac Amyloidosis: A Head-to-Head Comparison of Deformation and Nondeformation Parameters. *Circ Cardiovasc Imaging.* 2017;10(3):e005588. doi: 10.1161/CIRCIMAGING.116.005588.
27. Arvidsson S, Henein MY, Wikström G, Suhr OB, Lindqvist P. Right Ventricular Involvement in Transthyretin Amyloidosis. *Amyloid.* 2018;25(3):160-6. doi: 10.1080/13506129.2018.1493989.
28. Uzan C, Lairez O, Raud-Raynier P, Garcia R, Degand B, Christiaens LP, et al. Right Ventricular Longitudinal Strain: A Tool for Diagnosis and Prognosis in Light-Chain Amyloidosis. *Amyloid.* 2018;25(1):18-25. doi: 10.1080/13506129.2017.1417121.
29. Boldrini M, Cappelli F, Chacko L, Restrepo-Cordoba MA, Lopez-Sainz A, Giannoni A, et al. Multiparametric Echocardiography Scores for the Diagnosis of Cardiac Amyloidosis. *JACC Cardiovasc Imaging.* 2020;13(4):909-20. doi: 10.1016/j.jcmg.2019.10.011.
30. Aimo A, Chubuchny V, Vergaro G, Barison A, Nicol M, Cohen-Solal A, et al. A Simple Echocardiographic Score to Rule Out Cardiac Amyloidosis. *Eur J Clin Invest.* 2021;51(5):e13449. doi: 10.1111/eci.13449.
31. Davies DR, Redfield MM, Scott CG, Minamisawa M, Grogan M, Dispenzieri A, et al. A Simple Score to Identify Increased Risk of Transthyretin Amyloid Cardiomyopathy in Heart Failure with Preserved Ejection Fraction. *JAMA Cardiol.* 2022;7(10):1036-44. doi: 10.1001/jamacardio.2022.1781.
32. Nakao Y, Saito M, Inoue K, Higaki R, Yokomoto Y, Ogimoto A, et al. Cardiac Amyloidosis Screening Using a Relative Apical Sparing Pattern in Patients with Left Ventricular Hypertrophy. *Cardiovasc Ultrasound.* 2021;19(1):30. doi: 10.1186/s12947-021-00258-x.
33. Nicol M, Baudet M, Brun S, Harel S, Royer B, Vignon M, et al. Diagnostic Score of Cardiac Involvement in AL Amyloidosis. *Eur Heart J Cardiovasc Imaging.* 2020;21(5):542-8. doi: 10.1093/ehjci/jez180.
34. Alwan L, Benz DC, Cuddy SAM, Dobner S, Shiri I, Caobelli F, et al. Current and Evolving Multimodality Cardiac Imaging in Managing Transthyretin Amyloid Cardiomyopathy. *JACC Cardiovasc Imaging.* 2024;17(2):195-211. doi: 10.1016/j.jcmg.2023.10.010.
35. Goto S, Mahara K, Beussink-Nelson L, Ikura H, Katsumata Y, Endo J, et al. Artificial Intelligence-Enabled Fully Automated Detection of Cardiac Amyloidosis Using Electrocardiograms and Echocardiograms. *Nat Commun.* 2021;12(1):2726. doi: 10.1038/s41467-021-22877-8.
36. Goto S, Solanki D, John JE, Yagi R, Homilius M, Ichihara G, et al. Multinational Federated Learning Approach to Train ECG and Echocardiogram Models for Hypertrophic Cardiomyopathy Detection. *Circulation.* 2022;146(10):755-69. doi: 10.1161/CIRCULATIONAHA.121.058696.
37. Huda A, Castaño A, Niyogi A, Schumacher J, Stewart M, Bruno M, et al. A Machine Learning Model for Identifying Patients at Risk for Wild-Type Transthyretin Amyloid Cardiomyopathy. *Nat Commun.* 2021;12(1):2725. doi: 10.1038/s41467-021-22876-9.
38. Bonnefous L, Kharoubi M, Bézard M, Oghina S, Le Bras F, Pouillot E, et al. Assessing Cardiac Amyloidosis Subtypes by Unsupervised Phenotype Clustering Analysis. *J Am Coll Cardiol.* 2021;78(22):2177-92. doi: 10.1016/j.jacc.2021.09.858.

